



**RESEARCH ARTICLE**

**ALAMOUTI SPACE-TIME CODING FOR VEHICULAR COMMUNICATIONS IN THE  
PRESENCE OF CHANNEL ESTIMATION ERRORS**

Serdar Özgür ATA

TÜBİTAK BİLGEM, P.K. 74, 41470 Gebze, Kocaeli, [serdar.ata@tubitak.gov.tr](mailto:serdar.ata@tubitak.gov.tr), ORCID: 0000-0003-2902-6282

*Receive Date: 04.07.2023*

*Accepted Date: 12.07.2023*

**ABSTRACT**

In this paper, the error performance of the Alamouti space-time coding (STC) scheme is investigated for vehicle-to-vehicle (V2V) communication systems over imperfect cascaded fading channels. In vehicular communication systems, perfect knowledge of the channel state information is not available to the users at all times due to the rapid movement of communicating vehicles and fast change of the rich scattering environment which makes the fading effects in wireless channels more severe. Therefore, in the analysis, we consider the erroneous estimation of the channel gain, which is more realistic for practical scenarios. For this purpose, we first derive the moment-generation function (MGF) of the channel fading coefficient with estimation error in the case of the cascaded Nakagami- $m$  fading conditions. Then, using the MGF, we obtain the closed-form symbol-error-rate (SER) expressions of Alamouti STC with two transmitting and  $L$  receiving antennas for the M-PSK and M-QAM modulation schemes. Then, the exact ergodic capacity expression is derived for the proposed system. Furthermore, the analytical results are verified through Monte-Carlo simulations. Numerical results show that the SER performance of V2V communication systems can be improved significantly by using Alamouti STC even in case of harsh fading conditions and full channel-state information is not available due to estimation errors.

**Keywords:** *Alamouti Space-Time Coding, Cascaded Fading Channels, Channel Estimation Error, Ergodic Capacity, Symbol-Error Rate, Vehicular Communications*

**1. INTRODUCTION**

Vehicular communication is a rapidly growing research field of wireless communication applications with the potential to sustain safety, efficiency, and reliability in high-mobility environments in 5G networks. The focus on communications among vehicles or between vehicles and the infrastructure has been achieving high data rates, besides lower energy consumption and lower latency in 5G networks [1-3]. With the ultra-connectivity objective of 6G communications, seamless and secure communications is also aimed for intelligent transportation systems. Thus the internet of vehicles (IoV) is emerging as an advanced vehicular networking technology [4-6]. Moreover, the presence of dense and high-speed vehicles and the need for reliable and secure communication of a very high

number and density of communication nodes will increase the effective usage of artificial intelligence techniques in next-generation vehicular communication systems [7-8].

As the number of connected autonomous vehicles grows, vehicle-to-everything (V2X) communication technologies including vehicle-to-infrastructure communications (V2I), vehicle-to-vehicle (V2V) communications, vehicle-to-pedestrian (V2P) communications present intrinsic challenges for ensuring continuous and seamless connectivity [9]. The main challenge is the severe fading channel effects limiting the channel capacity. The channel effects become much more challenging in V2X systems as the receivers and transmitters are almost always in motion [10-11]. In addition, the presence of tall buildings and structures in urban areas or natural elevations and tall trees in rural areas cause shading effects. On the other hand, frequency spread due to Doppler shift at high speeds is another disturbance factor in V2X systems [12].

The channel fading effect in vehicular communication systems is modelled as cascaded channel models including Nakagami- $m$  fading model because the channel gains resulting from independent scattering fields are multiplied by each other to characterize the relevant statistical properties [13-14]. Several studies have been done to enhance the performance of V2V systems under Nakagami- $m$  fading. Two-way half-duplex amplify-and-forward (AF) relaying in vehicular communications was analysed in [15]. The fixed-gain AF relaying over cascaded Nakagami- $m$  channels with physical layer network coding was introduced in [16]. The performance analysis of full-duplex AF relaying over cascaded Nakagami- $m$  fading channels incorporating self-interference (SI) at the relay is studied in [17] for V2V communications.

In vehicular communications, due to the high-speed environment and insufficient pilot subcarriers in the symbols, channel estimation becomes a challenging task in practice for fast time-varying channels. Conventional channel estimation methods may not overcome error propagation problems and new compensation schemes are designed [18]. Moreover, channel estimation for high mobility systems is considered in [19] to extensively analyse the channel estimation performance where reconfigurable intelligent surfaces (RISs) are incorporated into the environment.

Moreover, space-time coding (STC) is a powerful technique used in wireless networks with multiple transmit antennas to improve the reliability of data transmission under severe channel conditions. Alamouti space-time coding has been extensively studied for wireless communication systems in urban environments [20]. The performance analysis on symbol-error-probability (SEP) in a multiple-relay AF cooperative communication system with Alamouti-type orthogonal STC at the transmitter and Alamouti's space-time-decoder at the receiver is investigated in [21] with imperfect channel-state-information (CSI). In [22], a new differential space-time block coded spatial modulation (STBC-SM) technique is introduced for multi-user massive multiple-input multiple-output (MIMO) communications in the uplink, where STBC-SM and differential coding is combined to strengthen the diversity gains in the absence of the CSI.

Hence, to fill in the gap in the investigation of how channel estimation errors affect the system performance of vehicular communication systems and to advance the error performance of V2V communication systems over cascaded fading channels in the presence of channel estimation errors,

we propose to use the Alamouti STBC technique using  $M$ -ary modulation schemes, then examine the performance of the proposed systems. The contributions of this paper are listed as follows.

- The MGF of erroneously estimated fading gain in the cascaded Nakagami- $m$  channels is derived in the closed form. Thus, for the first time in literature, we investigate the performance analysis of the V2V communication system subject to imperfect cascaded fading channels, which is more suitable for realistic wireless vehicular communication scenarios.
- A closed-form expression for the symbol-error-rate (SER) of Alamouti STC for M-PSK modulation over imprecise cascaded Nakagami- $m$  fading channels is obtained.
- The closed-form SER formulation of Alamouti STC for M-QAM modulation over imprecise cascaded Nakagami- $m$  fading channels is obtained.
- The closed-form average capacity expression of Alamouti STC over imprecise cascaded Nakagami- $m$  fading channels is obtained.

The rest of the paper is organized as follows. Section 2 introduces the proposed V2V communication system model. Section 3 presents the imperfect cascaded Nakagami- $m$  fading channel model. In Section 4, the derivation of the MGF of the channel gain with estimation errors and the MGF of the end-to-end SNR over imperfect cascaded Nakagami- $m$  fading channels are performed. Then, using these MGFs, SER expressions for the M-PSK and M-QAM modulation schemes are provided. In Section 5, ergodic capacity analysis is given. Section 6 represents the numerical and Monte-Carlo simulation results to verify the analytical derivations and discusses the performance of the proposed system. Finally, the contributions and findings of the paper are summarized in Section 7.

## 2. SYSTEM MODEL

Due to reasons such that the rapidly changing physical environment which consists of too many scattering obstacles, high mobility of the communicating nodes, and their lower antenna heights, fading conditions in V2V communication systems are much more severe compared to the classical wireless communication systems. Therefore, to enhance the error performance of these systems, the usage of diversity techniques is inevitable in designing the V2V communication infrastructures. At this point, as there is no space limitation on the vehicles, using the space-time diversity techniques by deploying multi-antennas on the nodes is a very reasonable choice. Providing full-rate and full diversity gain, no need for CSI or knowledge of channel coefficients at the transmitter, and having low implementation complexity with a simple decoding scheme, Alamouti STC can be very useful from a practical point of view to be used in vehicular communication systems illustrated in Figure 1. Additionally, since it requires just two consecutive time slots to transmit the source's signals, it also offers an adequate solution against the changeable characteristics of the vehicular channels. Thus, we examine a V2V communication system in Figure-1 where the  $2 \times L$  Alamouti STC is employed between the source with two transmitting antennas and the destination with  $L$  receiving antennas. Hence the source transmits two symbols  $s_1$  and  $s_2$  in the form of Alamouti code at time  $t$  and  $t + T$  by using two antennas as

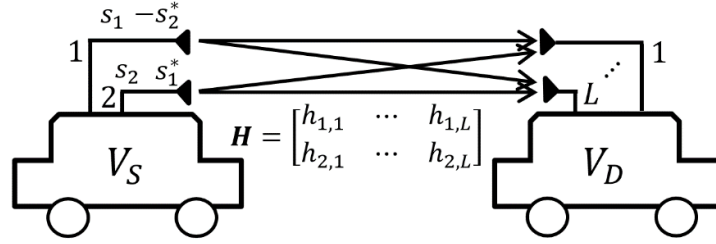


**Figure 1.** V2V communication system employing  $2 \times L$  Alamouti Space-Time Coding scheme, where  $V_S$  is the source vehicle,  $V_D$  is the destination vehicle, and  $\mathbf{H}$  is the channel gain matrix.

$$\mathbf{S} = \begin{bmatrix} s_1 & s_2 \\ -s_2^* & s_1^* \end{bmatrix}, \quad (1)$$

where  $\mathbf{S}$  is the code matrix for STC of Alamouti type and  $*$  denotes the complex conjugate operator. In  $\mathbf{S}$ , row indices indicate the transmitting time interval while column indices indicate which antenna is used to transmit the corresponding symbol in a given time interval [23]. Since the number of transmitting antennas  $n_T$  is 2 and receiving antennas  $n_R$  is  $L$ , the channel gain matrix,  $\mathbf{H}$ , becomes

$$\mathbf{H} = \begin{bmatrix} h_{1,1} & \dots & h_{1,L} \\ h_{2,1} & \dots & h_{2,L} \end{bmatrix}, \quad (2)$$

where  $h_{i,l}$  is the channel's fading coefficient between the  $i^{th}$  transmitting antenna of the source and the  $l^{th}$  receiving antenna of the destination, where  $i = 1, 2$  and  $l = 1, \dots, L$ . Therefore, after the transmission phase, signals received by the  $l^{th}$  antenna of the destination node at time  $t$  and  $t + T$  become

$$r_1^l = h_{1,l}s_1 + h_{2,l}s_2 + n_1^l, \quad (3a)$$

$$r_2^l = -h_{1,l}s_2^* + h_{2,l}s_1^* + n_2^l, \quad (3b)$$

respectively, where  $n_1^l$  and  $n_2^l$  denote the additive white Gaussian noise (AWGN) modelled as Gaussian random variables with zero mean and double-sided power spectral density of  $N_0/2$ . Then the receiver constructs two decision statistics  $\tilde{s}_1$  and  $\tilde{s}_2$  by combining the received signals with channels state information as [23]

$$\tilde{s}_1 = \sum_{l=1}^L h_{1,l}^* r_1^l + h_{2,l} (r_2^l)^* = \sum_{l=1}^L \sum_{k=1}^2 |h_{k,l}|^2 s_1 + \sum_{l=1}^L h_{1,l}^* n_1^l + h_{2,l} (n_2^l)^*, \quad (4)$$

$$\tilde{s}_2 = \sum_{l=1}^L h_{2,l}^* r_1^l - h_{1,l} (r_2^l)^* = \sum_{l=1}^L \sum_{k=1}^2 |h_{k,l}|^2 s_2 + \sum_{l=1}^L h_{2,l}^* n_1^l - h_{1,l} (n_2^l)^*. \quad (5)$$

After applying the maximum-combining-ratio (MRC) scheme to the received symbols, the instantaneous SNR per symbol becomes

$$\gamma = \sum_{l=1}^L \gamma_l = \sum_{l=1}^L \gamma_{1,l} + \gamma_{2,l} = \frac{P_s}{2N_0} \sum_{l=1}^L |h_{1,l}|^2 + |h_{2,l}|^2, \quad (6)$$

where  $P_s$  is the total transmitting power of the source node.

### 3. CHANNEL MODEL

In cascaded fading channel models, the channel gain  $h$  is modeled as the multiplication of several random variables  $\{h_n\}_{n=1}^N$ , which correspond to the multiple scattering effects in the medium as [13]

$$h = \prod_{n=1}^N h_n, \quad (7)$$

where  $N$  denotes the cascading degree of the wireless channel. For the case of  $h_n$  being a Nakagami- $m$  distributed random variable with the fading parameter of  $m_n$ , it is called as  $N^*$ Nakagami- $m$  fading channel and probability density function (PDF) besides cumulative distribution function (CDF) of  $h$  are given as [13]

$$f_h(h) = 2h^{-1} \delta G_{0,N}^{N,0} \left[ h^2 \Delta \mid \begin{matrix} (-), (-) \\ (m_1, \dots, m_N), (-) \end{matrix} \right], \quad (8a)$$

$$F_h(h) = \delta G_{1,N+1}^{N,1} \left[ h^2 \Delta \mid \begin{matrix} (1), (-) \\ (m_1, \dots, m_N), (0) \end{matrix} \right], \quad (8b)$$

where  $\delta = \prod_{n=1}^N (1/\Gamma(m_n))$  and  $\Delta = \prod_{n=1}^N (m_n/\Omega_n)$  while  $\{\Omega_n\}_{n=1}^N$  is the average power of the corresponding multiplicative channel gain as  $\Omega_n = E[h_n^2]$ , where  $E[\cdot]$  denotes the expectation operator. Here  $\Gamma(\cdot)$  is Gamma function [24, 8.310] and  $G_{v,u}^{s,t} \left[ \cdot \mid \begin{matrix} \underline{a}_t, \underline{a}_v \\ \underline{b}_s, \underline{b}_u \end{matrix} \right]$  is the Meijer's G function [24, 9.301], where  $\underline{a}_t \triangleq (a_1, \dots, a_t)$ ,  $\underline{a}_v \triangleq (a_{t+1}, \dots, a_v)$ ,  $\underline{b}_s \triangleq (b_1, \dots, b_s)$ , and  $\underline{b}_u \triangleq (b_{s+1}, \dots, b_u)$ .

In vehicular communications, due to the rapid movement of the communicating nodes and rich scattering environment, fading characteristics of the wireless channels may vary fast in time and therefore the perfect estimation of the channel statistics may not be possible. For these reasons, assuming imperfect channel estimation is much more reasonable in practical V2V application scenarios. In that case, the erroneously estimated channel gain  $\hat{h}$  can be modelled as a summation of the perfectly estimated channel gain  $h$  and an error term  $n_h$ , and mathematically given as [21]

$$\hat{h} = \rho h + \sqrt{1 - \rho^2} n_h, \quad (9)$$

where  $\rho$  is the correlation coefficient between  $h$  and  $\hat{h}$ , holding  $0 \leq \rho \leq 1$ , which determines the accuracy of the estimation. Furthermore, the estimation error  $n_h$  is normally distributed with zero mean and  $\sigma_h^2$  variance,  $n_h \sim N(0, \sigma_h^2)$ .

#### 4. PERFORMANCE EVALUATION

In the letter, the performance analysis of the proposed system is evaluated by exploiting the moment generation function (MGF) approach. With the definitions of  $\alpha \triangleq \rho h$  and  $\beta \triangleq \sqrt{1 - \rho^2} n_h$ , then  $\hat{h} = \alpha + \beta$ , it can be written that

$$\gamma \triangleq \hat{h}^2 = \alpha^2 + 2\alpha\beta + \beta^2. \quad (10)$$

Thus, the MGF of  $Y$ , which is denoted by  $\mathcal{M}_Y(s)$ , becomes

$$\mathcal{M}_Y(s) = E[e^{-sY}] = E[e^{-s\alpha^2} e^{-s\beta^2} e^{-2s\alpha\beta}]. \quad (11)$$

By using the  $K - th$  order Taylor expansion of the term  $e^{-2s\alpha\beta}$ ,  $\mathcal{M}_Y(s)$  can be written as

$$\begin{aligned} \mathcal{M}_Y(s) &= E \left[ e^{-s\alpha^2} e^{-s\beta^2} \sum_{k=0}^K \frac{(-2s)^k}{k!} \alpha^k \beta^k \right] \\ &= \sum_{k=0}^K \frac{(-2s)^k}{k!} E[e^{-s\alpha^2} \alpha^k] E[e^{-s\beta^2} \beta^k] \\ &= \sum_{k=0}^K \frac{(-2s)^k}{k!} I_\alpha(s) I_\beta(s), \end{aligned} \quad (12)$$

where

$$I_\alpha(s) = E[e^{-s\alpha^2} \alpha^k] = \int_0^\infty e^{-s\alpha^2} \alpha^k f_\alpha(\alpha) d\alpha \quad (13)$$

and

$$I_\beta(s) = E[e^{-s\beta^2} \beta^k] = \int_{-\infty}^\infty e^{-s\beta^2} \beta^k f_\beta(\beta) d\beta. \quad (14)$$

Since  $f_\alpha(\alpha) = \rho^{-1} f_h(\alpha/\rho)$ , by using (8a),  $I_\alpha(s)$  can be written as

$$I_\alpha(s) = 2\delta \int_0^\infty e^{-s\alpha^2} \alpha^{k-1} G_{0,N}^{N,0} \left[ \alpha^2 \frac{\Delta}{\rho^2} \mid \begin{matrix} (-),(-) \\ (m_1, \dots, m_N), (-) \end{matrix} \right] d\alpha. \quad (15)$$

Then, by applying  $z = \alpha^2$  transformation, this integral can take the form of

$$I_\alpha(s) = \delta \int_0^\infty e^{-sz} z^{\frac{k}{2}-1} G_{0,N}^{N,0} \left[ z \frac{\Delta}{\rho^2} \mid \begin{matrix} (-),(-) \\ (m_1, \dots, m_N), (-) \end{matrix} \right] dz \quad (16)$$

and exploiting the integral property of Meijer's G function [25, 2.24.3.1],  $I_\alpha(s)$  is obtained as

$$I_\alpha(s) = \delta S^{\frac{k}{2}} G_{1,N}^{N,1} \left[ \frac{\Delta}{s\rho^2} \mid \begin{matrix} (1-\frac{k}{2}),(-) \\ (m_1, \dots, m_N), (-) \end{matrix} \right]. \quad (17)$$

After that, by following a similar approach, using the relation of  $f_{\beta}(\beta) = f_{n_h}(\beta/\sqrt{1-\rho^2})/\sqrt{1-\rho^2}$  and after several algebraic manipulations,  $I_{\beta}(s)$  may be reformulated as

$$I_{\beta}(s) = \xi \int_{-\infty}^{\infty} e^{-(s+\Xi)\beta^2} \beta^k d\beta, \quad (18)$$

where  $\xi = 1/\sqrt{2\pi\sigma^2(1-\rho^2)}$  and  $\Xi = (2\sigma^2(1-\rho^2))^{-1}$ . Then, with the help of [24, 3.383.11],  $I_{\beta}(s)$  is obtained as

$$I_{\beta}(s) = \frac{\xi}{(s+\Xi)^{\frac{k+1}{2}}} \Gamma\left(\frac{k+1}{2}\right). \quad (19)$$

Hence, by substituting (17) and (19) into (12),  $M_{\gamma}(s)$  is obtained as

$$\mathcal{M}_{\gamma}(s) = \xi \delta \sum_{k=0}^K \frac{(-2s)^k}{k!} \frac{\Gamma\left(\frac{k+1}{2}\right)}{(s+\Xi)^{\frac{k+1}{2}}} S^{\frac{k}{2}} G_{1,N}^{N,1} \left[ \frac{\Delta}{s\rho^2} \mid \begin{matrix} (1-\frac{k}{2}), (-) \\ (m_1, \dots, m_N), (-) \end{matrix} \right]. \quad (20)$$

Now, by defining the instantaneous SNR in the imperfect cascaded fading channel as  $\gamma \stackrel{\Delta}{=} \bar{\gamma}Y$ , it holds that

$$\mathcal{M}_{\gamma}(s) = E[e^{-s\gamma}] = E[e^{-s\bar{\gamma}Y}] = \mathcal{M}_{\gamma}(s\bar{\gamma}), \quad (21)$$

where  $\bar{\gamma}$  is denoting the average SNR at a fading channel and defined as  $\bar{\gamma} = P/2N_0$ , while  $P$  is the total transmitting power of the source node. Hence, by substituting  $s\bar{\gamma}$  into (20), the MGF of  $\gamma$  is obtained as

$$\mathcal{M}_{\gamma}(s) = \xi \delta \sum_{k=0}^K \frac{(-2)^k \Gamma\left(\frac{k+1}{2}\right)}{k!} \frac{(s\bar{\gamma})^{\frac{3k}{2}}}{(s\bar{\gamma}+\Xi)^{\frac{k+1}{2}}} G_{1,N}^{N,1} \left[ \frac{\Delta}{s\bar{\gamma}\rho^2} \mid \begin{matrix} (1-\frac{k}{2}), (-) \\ (m_1, \dots, m_N), (-) \end{matrix} \right]. \quad (22)$$

#### 4.1. $2 \times 1$ Alamouti STC Scheme

In the case of the systems consisting of a source with two transmitting antennas and a destination with a single receiving antenna,  $L = 1$ , end-to-end SNR denoted by  $\gamma_T$  at the destination is

$$\gamma_T = \gamma_1 + \gamma_2, \quad (23)$$

therefore, the MGF of  $\gamma_T$  becomes

$$\mathcal{M}_{\gamma_T}(s) = \mathcal{M}_{\gamma_1}(s) \mathcal{M}_{\gamma_2}(s), \quad (24)$$

where the  $\mathcal{M}_{\gamma_i}(s)$ , for  $i \in \{1, 2\}$ , is calculated with the help of (22) by using the corresponding channel parameters as  $(\rho, N, m_n, \Omega_n, \sigma, \xi, \delta, \Xi, \Delta) \rightarrow (\rho_i, N_i, m_{n,i}, \Omega_{n,i}, \sigma_i, \xi_i, \delta_i, \Xi_i, \Delta_i)$ .

#### 4.2. $2 \times L$ Alamouti STC Scheme

In case of  $L$  receiving antennas installed at the destination vehicle, the instantaneous SNR at the  $l^{th}$  antenna is

$$\gamma_l = \gamma_{l,1} + \gamma_{l,2} \quad (25)$$

and the corresponding MGF becomes

$$\mathcal{M}_{\gamma_l}(s) = \mathcal{M}_{\gamma_{l,1}}(s)\mathcal{M}_{\gamma_{l,2}}(s). \quad (26)$$

Thus, the end-to-end SNR acquired by the destination after employing the MRC scheme is obtained as

$$\gamma_T = \sum_{l=1}^L \gamma_l \quad (27)$$

and the MGF of  $\gamma_T$  can be calculated as

$$\mathcal{M}_{\gamma_T}(s) = \prod_{l=1}^L \mathcal{M}_{\gamma_l}(s). \quad (28)$$

Yet again, while evaluating (28) via (26), calculation of  $\mathcal{M}_{\gamma_{l,i}}(s)$ , for  $i \in \{1, 2\}$  is performed by using (22) with the corresponding channel parameters as  $(\rho, N, m_n, \Omega_n, \sigma, \xi, \delta, \Xi, \Delta) \rightarrow (\rho_i^l, N_i^l, m_{n,i}^l, \Omega_{n,i}^l, \sigma_i^l, \xi_i^l, \delta_i^l, \Xi_i^l, \Delta_i^l)$  between the  $i^{th}$  transmitting and the  $l^{th}$  receiving antennas.

#### 4.3. Symbol-Error-Rate for M-PSK Modulation

When considering an  $L$ -branch MRC receiver, the average SER for M-PSK modulation over generalized fading channels is given by

$$P_e^{M-PSK} = \frac{1}{\pi} \int_0^{\pi-\pi/M} \mathcal{M}_{\gamma_T}(\theta_M) d\theta = \frac{1}{\pi} \int_0^{\pi-\pi/M} \prod_{l=1}^L \mathcal{M}_{\gamma_l}(\theta_M) d\theta, \quad (29)$$

where  $\theta_M = \frac{\sin^2(\pi/M)}{\sin^2\theta}$  [26]. Even though an explicit solution of (29) in terms of elementary functions has not been derived due to the integral expression of the multiplication of  $L$  Meijer's G functions, which is not tabulated in the current literature, a tight approximation for SER of the M-PSK modulation can be effectively calculated as [27]

$$P_e^{M-PSK} \approx \left(\frac{1}{3} - \frac{1}{2M}\right) \mathcal{M}_{\gamma_T}\left(\sin^2\left(\frac{\pi}{M}\right)\right) + \frac{1}{4} \mathcal{M}_{\gamma_T}\left(\frac{4}{3} \sin^2\left(\frac{\pi}{M}\right)\right) + \left(\frac{1}{4} - \frac{1}{2M}\right) \mathcal{M}_{\gamma_T}\left(\frac{\sin^2\left(\frac{\pi}{M}\right)}{\sin^2\left(\pi - \frac{\pi}{M}\right)}\right). \quad (30)$$

Thus, by substituting (28) into (30) and using the MGF expression of the instantaneous SNR in cascaded fading channels with estimation errors in (22), the average symbol error rate of Alamouti STC using M-PSK modulation is obtained for V2V communication systems over  $N^*$ Nakagami- $m$  fading channels with channel estimation error.

#### 4.4. Symbol-Error-Rate for M-QAM Modulation

The average SER for a coherent M-QAM modulation scheme with multi-channel reception is given as

$$P_e^{M-QAM} = \frac{4\alpha}{\pi} \int_0^{\pi/2} \mathcal{M}_{\gamma_T}(\phi_M) d\phi - \frac{4\alpha^2}{\pi} \int_0^{\pi/4} \mathcal{M}_{\gamma_T}(\phi_M) d\phi, \quad (31)$$

where  $\alpha = \left(1 - \frac{1}{M}\right)$  and  $\phi_M = \frac{3/(2(M-1))}{\sin^2 \phi}$  [26]. Using the relation between the expectation operation and the MGF function, (31) can be written as

$$P_e^{M-QAM} = E[I_1] - E[I_2], \quad (32)$$

where  $I_1$  and  $I_2$  are the integral expressions of

$$I_1 = \frac{4\alpha}{\pi} \int_0^{\pi/2} e^{-\phi_{M\gamma_T}} d\phi, \quad (33a)$$

$$I_2 = \frac{4\alpha^2}{\pi} \int_0^{\pi/4} e^{-\phi_{M\gamma_T}} d\phi, \quad (33b)$$

respectively. With the help of [27, Eq.8],  $I_1$  can be approximated as

$$I_1 \approx 4\alpha \left( \frac{1}{12} e^{-\phi_{M\gamma_T}} + \frac{1}{4} e^{-\frac{4}{3}\phi_{M\gamma_T}} \right) = \frac{\alpha}{3} e^{-\phi_{M\gamma_T}} + \alpha e^{-\frac{4}{3}\phi_{M\gamma_T}}, \quad (34)$$

therefore  $E[I_1]$  becomes

$$E[I_1] \approx \frac{\alpha}{3} \mathcal{M}_{\gamma_T} \left( \frac{3}{2(M-1)} \right) + \alpha \mathcal{M}_{\gamma_T} \left( \frac{2}{M-1} \right). \quad (35)$$

For the derivation of  $E[I_2]$ , we can write

$$E[I_2] = E[I_{21}] - E[I_{22}], \quad (36)$$

where

$$I_{21} = \frac{4\alpha^2}{\pi} \int_0^{\pi/2} e^{-\phi_{M\gamma_T}} d\phi, \quad (37a)$$

$$I_{22} = \frac{4\alpha^2}{\pi} \int_{\pi/4}^{\pi/2} e^{-\phi_{M\gamma_T}} d\phi. \quad (37b)$$

Similarly, with the help of [27, Eq.8],  $I_{21}$  can be approximated as

$$I_{21} \approx 4\alpha^2 \left( \frac{1}{12} e^{-\phi_{M\gamma_T}} + \frac{1}{4} e^{-\frac{4}{3}\phi_{M\gamma_T}} \right) = \frac{\alpha^2}{3} e^{-\phi_{M\gamma_T}} + \alpha^2 e^{-\frac{4}{3}\phi_{M\gamma_T}}, \quad (38)$$

then

$$E[I_{21}] \approx \frac{\alpha^2}{3} \mathcal{M}_{\gamma_T} \left( \frac{3}{2(M-1)} \right) + \alpha^2 \mathcal{M}_{\gamma_T} \left( \frac{2}{M-1} \right). \quad (39)$$

In the evaluation of  $E[I_{22}]$ , by following the similar approach in [27] and using the trapezoid rule of the definite integrals, the integral expression of  $I_{22}$  can be approximated to the  $\left(\frac{4\alpha^2}{\pi}\right)$  times the area of a trapezoid having parallel sides of length with  $e^{-\frac{3}{2M-1}\frac{\gamma_T}{M-1}}$  and  $e^{-3\frac{\gamma_T}{M-1}}$ , and height with  $\left(\frac{\pi}{4}\right)$  as

$$I_{22} \approx \frac{4\alpha^2}{\pi} \left( e^{-\frac{3}{2M-1}\frac{\gamma_T}{M-1}} + e^{-3\frac{\gamma_T}{M-1}} \right) \frac{\pi}{8} = \frac{\alpha^2}{2} \left( e^{-\frac{3}{2M-1}\frac{\gamma_T}{M-1}} + e^{-3\frac{\gamma_T}{M-1}} \right) \quad (40)$$

and therefore  $E[I_{22}]$  is obtained as

$$E[I_{22}] \approx \frac{\alpha^2}{2} \mathcal{M}_{\gamma_T} \left( \frac{3}{2(M-1)} \right) + \frac{\alpha^2}{2} \mathcal{M}_{\gamma_T} \left( \frac{3}{M-1} \right). \quad (41)$$

By substituting (39) and (41),  $E[I_2]$  becomes

$$E[I_2] \approx \alpha^2 \mathcal{M}_{\gamma_T} \left( \frac{2}{M-1} \right) - \frac{\alpha^2}{2} \mathcal{M}_{\gamma_T} \left( \frac{3}{M-1} \right) - \frac{\alpha^2}{6} \mathcal{M}_{\gamma_T} \left( \frac{3}{2(M-1)} \right). \quad (42)$$

Finally, substituting (35) and (42) in (31), the average SER for a coherent M-QAM modulation scheme with multi-channel reception is obtained as

$$P_e^{M-QAM} \approx \left( \frac{1}{2} + \frac{1}{6M^2} \right) \mathcal{M}_{\gamma_T} \left( \frac{3}{2(M-1)} \right) + \frac{(M-1)^2}{2M^2} \mathcal{M}_{\gamma_T} \left( \frac{3}{M-1} \right) + \left( \frac{M-1}{M^2} \right) \mathcal{M}_{\gamma_T} \left( \frac{2}{M-1} \right). \quad (43)$$

Hence, by substituting (28) into (43) and then using (22), the average SER of Alamouti STC using M-QAM modulation is obtained for V2V communication systems that are subject to cascaded Nakagami- $m$  fading channels with channel estimation errors.

## 5. ERGODIC CAPACITY ANALYSIS

The exact ergodic capacity of  $L$ -branch diversity combiner over mutually not-necessarily independent or identically distributed fading channels is given by [28]

$$C_{avg} = \frac{W}{\log(2)} \sum_{n=1}^N w_n C_1(s_n) \frac{d}{ds} \mathcal{M}_{\gamma_T}(s) \Big|_{s \rightarrow s_n}, \quad (44)$$

where  $W$  is the channel's bandwidth,  $s_n = \tan\left(\frac{\pi}{4} \cos\left(\frac{2n-1}{2N}\pi\right) + \frac{\pi}{4}\right)$ , and  $w_n = \frac{\pi^2 \sin\left(\frac{2n-1}{2N}\pi\right)}{4N \cos^2\left(\frac{\pi}{4} \cos\left(\frac{2n-1}{2N}\pi\right) + \frac{\pi}{4}\right)}$ .

Using (26) and (28), it may be written that

$$\begin{aligned} \frac{d}{ds} \mathcal{M}_{\gamma_T}(s) &= \sum_{l=1}^L \prod_{j=1, j \neq l}^L \mathcal{M}_{\gamma_j}(s) \frac{d}{ds} \mathcal{M}_{\gamma_l}(s) \\ &= \sum_{l=1}^L \prod_{j=1, j \neq l}^L \mathcal{M}_{\gamma_j}(s) \times \left( \mathcal{M}_{\gamma_{l,2}}(s) \frac{d}{ds} \mathcal{M}_{\gamma_{l,1}}(s) + \mathcal{M}_{\gamma_{l,1}}(s) \frac{d}{ds} \mathcal{M}_{\gamma_{l,2}}(s) \right). \end{aligned} \quad (45)$$

By using (21), it may be written that  $\frac{d}{ds} \mathcal{M}_{\gamma_{l,i}}(s) = \bar{\gamma} \frac{d}{ds} \mathcal{M}_{\gamma}(s\bar{\gamma})$  where  $\bar{\gamma} = E[\gamma_{l,i}]$  for  $i \in 1, 2$ . Therefore,  $\frac{d}{ds} \mathcal{M}_{\gamma}(s)$  should be derived to calculate (45). Hence, by using (21)

$$\begin{aligned} \frac{d}{ds} \mathcal{M}_{\gamma}(s) &= \sum_{k=0}^K \frac{(-2s)^k}{k!} I_{\alpha}(s) I_{\beta}(s) \\ &= \sum_{k=0}^K \frac{(-2)^k}{k!} s^{k-1} \left( k I_{\alpha}(s) I_{\beta}(s) + s I_{\beta}(s) \frac{d}{ds} I_{\alpha}(s) + s I_{\alpha}(s) \frac{d}{ds} I_{\beta}(s) \right), \end{aligned} \quad (46)$$

where  $I_{\alpha}(s)$  and  $I_{\beta}(s)$  are given by (16) and (19), respectively. By using (16) it may be written as

$$\begin{aligned} \frac{d}{ds} I_{\alpha}(s) &= \frac{d}{ds} \delta \int_0^{\infty} e^{-sz} z^{\frac{k}{2}-1} G_{0,N}^{N,0} \left[ z \frac{\Delta}{\rho^2} \mid \begin{matrix} (-), (-) \\ (m_1, \dots, m_N), (-) \end{matrix} \right] dz \\ &= -\delta \int_0^{\infty} e^{-sz} z^{\frac{k}{2}} G_{0,N}^{N,0} \left[ z \frac{\Delta}{\rho^2} \mid \begin{matrix} (-), (-) \\ (m_1, \dots, m_N), (-) \end{matrix} \right] dz. \end{aligned} \quad (47)$$

Hence, with the help of the integral property of Meijer's G function [25, 2.24.3.1], (47) is obtained as

$$\frac{d}{ds} I_{\alpha}(s) = -\delta s^{\frac{k}{2}+1} G_{1,N}^{N,1} \left[ \frac{\Delta}{s\rho^2} \mid \begin{matrix} (-\frac{k}{2}), (-) \\ (m_1, \dots, m_N), (-) \end{matrix} \right]. \quad (48)$$

After that, by using (19)  $\frac{d}{ds} I_{\beta}(s)$  may be derived as

$$\frac{d}{ds} I_{\beta}(s) = \xi \Gamma\left(\frac{k+1}{2}\right) \frac{d}{ds} (s + \Xi)^{-\frac{k+1}{2}} = -\frac{k+1}{2} \xi \Gamma\left(\frac{k+1}{2}\right) (s + \Xi)^{-\frac{k+3}{2}}. \quad (49)$$

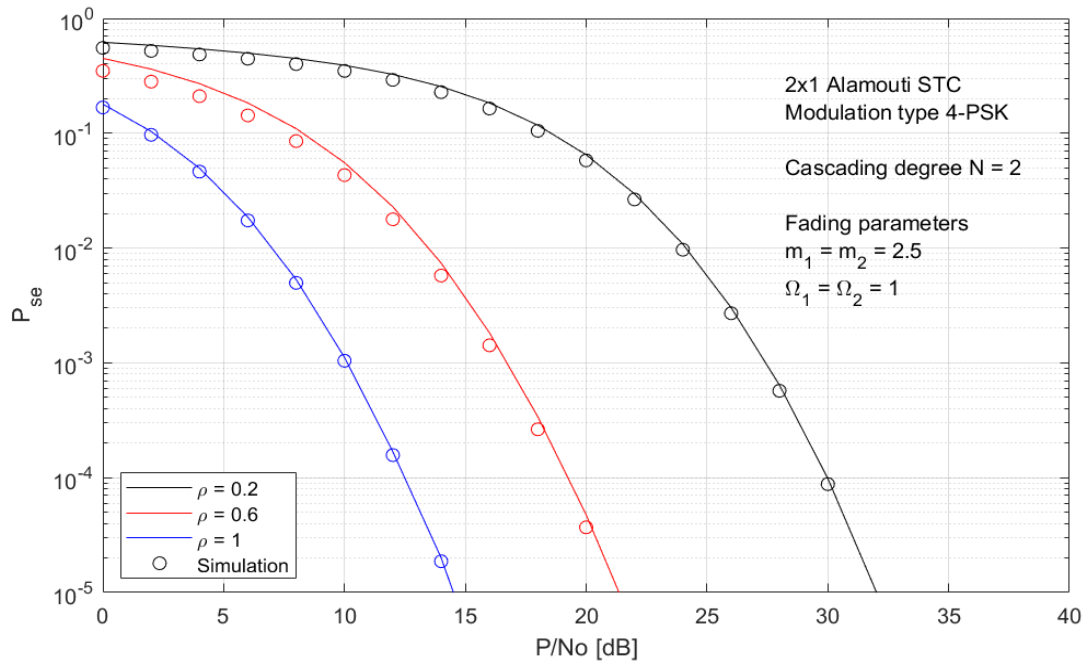


**Figure 2.** Performance of 2x1 Alamouti STBC over imprecise 2\*Nakagami- $m$  fading channels with  $m_1 = m_2 = 2.5$  for  $\rho = 0.2, 0.6,$  and  $1$ .

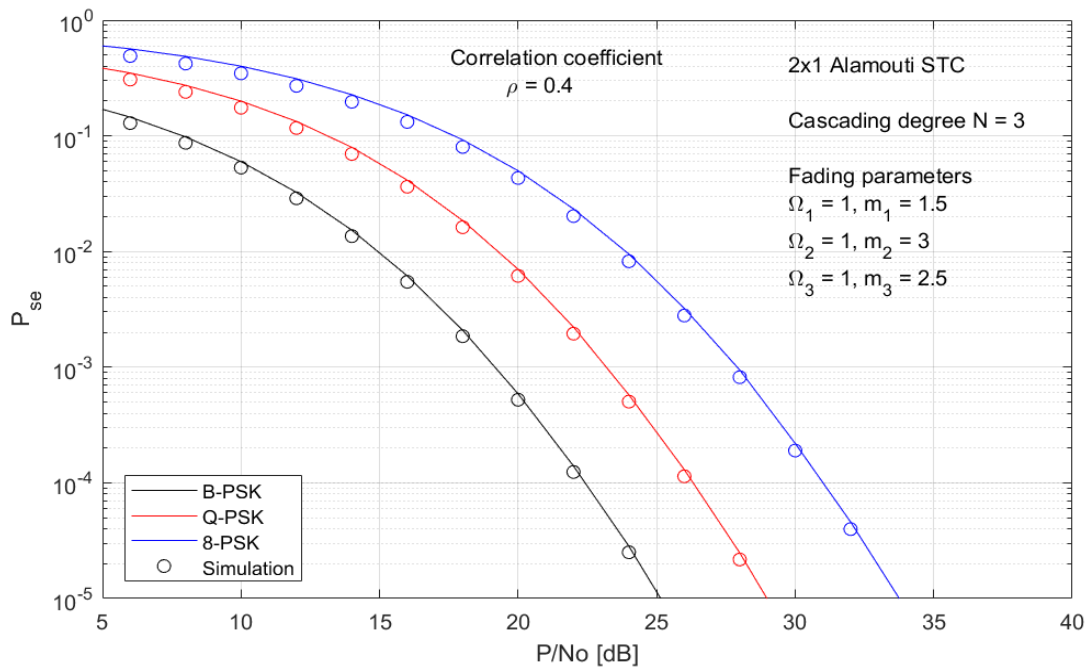
Thus, by substituting (48) and (49) into (46), then by calculating (45) with the help of (46) and substituting it into (44), the average capacity of the Alamouti STBC errors is obtained in the closed-form for MIMO V2V communication systems over cascaded fading channels with the channel estimation.

## 6. NUMERICAL RESULTS AND SIMULATIONS

Throughout this section, numerical results and simulations are provided comparatively to validate the analytic results derived in the paper. During calculations, it is assumed that the transmitter transmits the symbols with unit power per antenna. Also, the fading coefficients for the cascaded channels have unit power as  $\Omega = E[h^2]$ . In figures, the analytic plots are represented by solid lines while the simulation results are marked by circles.

In Figure 2, the SER performance of 2x1 Alamouti STBC using 4-PSK modulation over cascaded Nakagami- $m$  fading channels is presented for the miscellaneous degrees of channel estimation errors. For this figure, the cascading degree and the related fading parameters are set as  $N = 2$  and  $m_1 = m_2 = 2.5$ , respectively. The correlation coefficient between a channel gain  $h$  and its erroneous estimation  $\hat{h}$  is chosen as  $\rho \in \{0.2, 0.6, 1\}$ . As is seen from the figure, the presence of channel

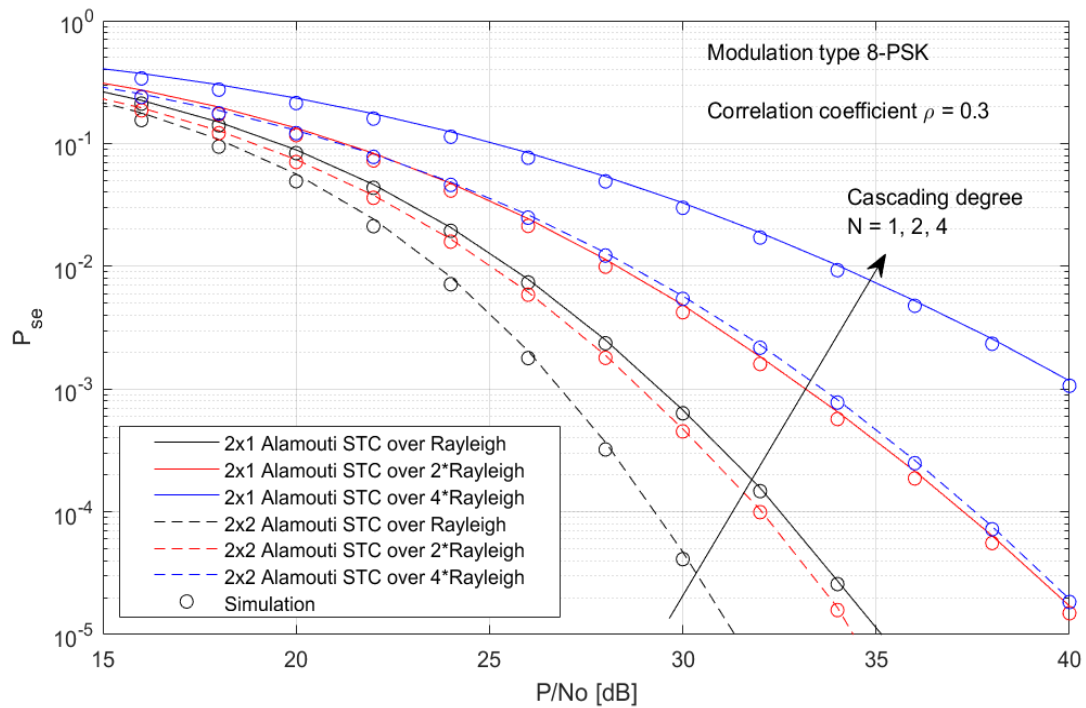
estimation errors significantly worsens the SER performance of the system. For example, to achieve  $10^{-3}$  error rate, an extra 7dB SNR is required for  $\rho = 0.6$  in comparison with the perfect estimation of the channel statistics which corresponds to  $\rho = 1$ .



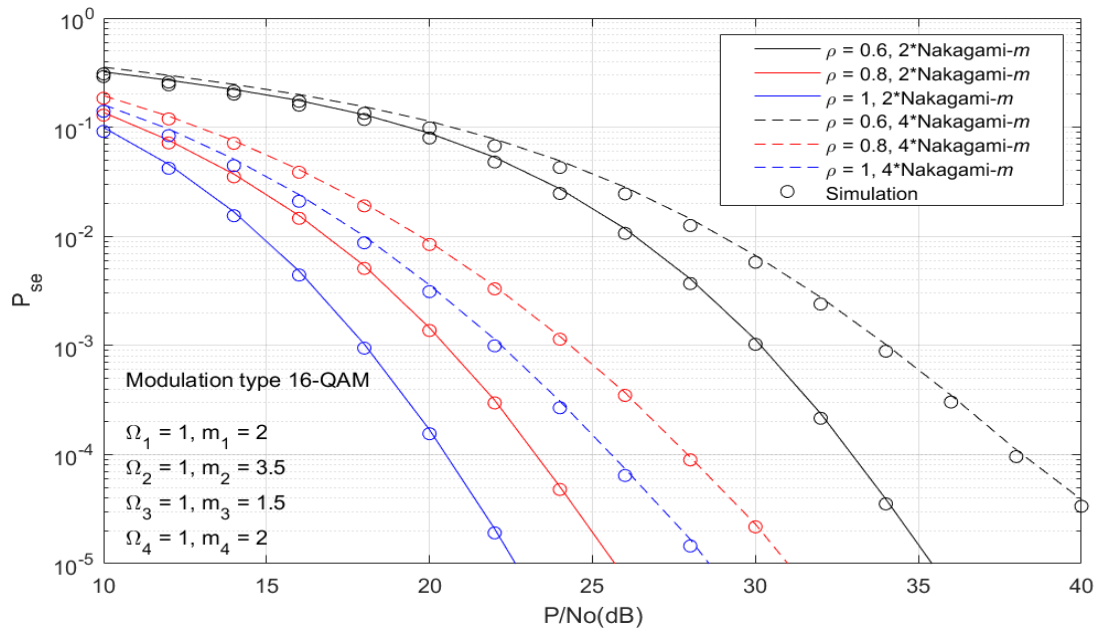
**Figure 3.** SER performances of vehicular communication systems employing Alamouti STC scheme with B/Q/8-PSK modulations over 3\*Nakagami- $m$  channels with  $m_1 = 1.5$ ,  $m_2 = 3$  and  $m_3 = 2.5$  in the presence of channel estimation errors for  $\rho = 0.4$ .

Figure 3 represents the effect of modulation order on the SER performance of Alamouti STC scheme over cascaded fading channels. The plots are given for the BPSK, QPSK, and 8-PSK modulation schemes over 3\*Nakagami- $m$  fading channels,  $N=3$ , with  $m_1 = 1.5$ ,  $m_2 = 3$ , and  $m_3 = 2.5$ . The correlation coefficient related to the estimation error is set as  $\rho = 0.4$ . As seen from the figure, the SER performance of the system decreases by increasing modulation order, which makes the maximum-likelihood decision-making process becomes more vulnerable to estimation errors since the distances among the symbols in the constellation are getting closer. For example, the figure shows that the SNR gap between BPSK and QPSK modulations is approximately 5dB at  $10^{-3}$  SER value. It is also seen that the 8-PSK modulation scheme requires extra 8dB SNR to provide the same SER value for the proposed system when compared with using BPSK modulation.

In Figure 4, the effect of the channel's cascading degree on the SER performances is presented when the cascading degree is as  $N = 1, 2$ , and  $4$ , which are corresponding to Rayleigh,  $2^*$ Rayleigh, and  $4^*$ Rayleigh fading channels, respectively, in V2V communication systems employing Alamouti's space-time coding scheme using 8-PSK modulation. Here, the correlation coefficient between  $h$  and  $\hat{h}$  is set as  $\rho = 0.3$ . The figure reveals that the increasing cascading degree of the fading channels significantly degrades the SER performance of the system. For example, the SNR gap between  $N = 1$  and  $N = 2$  (Rayleigh and  $2^*$ Rayleigh channels) is approximately  $5\text{dB}$  while it is about  $8\text{dB}$  in the case of  $N = 2$  and  $N = 4$  ( $2^*$ Rayleigh and  $4^*$ Rayleigh channels) to reach the  $10^{-3}$  SER value.



**Figure 4.** SER performances of vehicular communication systems employing Alamouti STBC using 8-PSK modulation for different vehicular fading channel models for  $\rho = 0.3$ .



**Figure 5.** Performances of Alamouti STC scheme using 16-QAM modulation over 2\*Nakagami- $m$  and 4\*Nakagami- $m$  fading channels for  $\rho = 0.6, 0.8,$  and  $1$ .

Additionally, Figure 4 represents the SER performance comparison for SIMO (2x1) and MIMO (2x2) configurations of Alamouti STBC over the imprecise cascaded Nakagami- $m$  fading channels. The figure reveals that the system performance may be significantly enhanced by using multiple receiving antennas. For example, an extra receiving antenna provides 10 times better SER at 30dB SNR.

The performance of Alamouti STC scheme using 16-QAM modulation for V2V communication systems is presented in Figure 5. The plots are given for 2\*Nakagami- $m$  with  $m_1 = 2, m_2 = 3.5,$  and 4\*Nakagami- $m$  with  $m_1 = 2, m_2 = 3.5, m_3 = 1.5, m_4 = 2$  fading channels and  $\rho = 0.6, 0.8, 1$  values of the correlation coefficient between  $h$  and its erroneous estimation  $\hat{h}$ . The figure reveals that the presence of channel estimation errors severely worsens the SER performance of vehicular communication systems. For example, to achieve the error rate of  $10^{-3}$  over 2\*Rayleigh fading channels, extra 13dB SNR is required for  $\rho = 0.6$  in comparison with the perfect estimation case in which  $\rho = 1$ . It is also seen that the PSK modulation provides better SER performance than the QAM modulation does in V2V communication systems employing Alamouti STBC over imprecise cascaded fading channels. Finally, it is shown by the figures that the analytical and simulation results tightly match, which is because of the analytical SER expressions are approximations to the exact ones.

## 7. CONCLUSIONS

In this letter, we proposed to use the Alamouti STC to enhance the SER performance of V2V communication systems over cascaded fading channels where the perfect knowledge of the channel state information is not available to the users all the time due to the rapid movement of the communicating vehicles and fast-changing characteristics of the rich scattering environment which makes the fading effects in wireless channels more severe. Therefore, in investigating the SER profile of the proposed system, we consider the erroneous estimation of the fading channels' gains which is much more realistic for the practical scenarios. During the analysis, we first derive the moment-generation function (MGF) of the erroneously estimated channel fading coefficient in the case of the cascaded Nakagami- $m$  fading conditions. Then, using this MGF, SER expressions of Alamouti STC with two transmitting and  $L$  receiving antennas for the M-PSK and M-QAM modulation schemes are obtained. After that the ergodic capacity analysis for the proposed system is examined and a closed-form expression of it is derived. Furthermore, the analytical results are verified by Monte-Carlo simulations. The results reveal that the SER performance of V2V communication systems is severely degraded in case of full channel-state information is not available due to estimation errors but it can be improved significantly by using the Alamouti STC method. It is also presented that using PSK modulation provides better SER performance than using QAM modulation in the vehicular communication systems employing Alamouti STC over imprecise cascaded fading channels.

## ACKNOWLEDGEMENT

This research received no specific grants from any public, commercial or non-profit funding agencies.

## REFERENCES

- [1] Gyawali, S., Xu, S., Qian, Y. and Hu, R.Q., (2021). Challenges and Solutions for Cellular Based V2X Communications, *IEEE Communications Surveys and Tutorials*, 23-1, 222-255.
- [2] Kim, J., Choi, Y.-J., Noh, G. and Chung, H., (2023). On the Feasibility of Remote Driving Applications Over mmWave 5G Vehicular Communications: Implementation and Demonstration, *IEEE Transactions on Vehicular Technology*, 72-2, 2009-2023.
- [3] Guo, C., Liang, L. and Li, G.Y., (2019). Resource Allocation for Vehicular Communications with Low Latency and High Reliability, *IEEE Transactions on Wireless Communications*, 18-8, 3887-3902.
- [4] Liu, R., Liu, A., Qu, Z. and Xiong, N.N., (2023). An UAV-Enabled Intelligent Connected Transportation System with 6G Communications for Internet of Vehicles, *IEEE Transactions on Intelligent Transportation Systems*, 24-2, 2045-2059.
- [5] Lv, Z., Qiao, L. and You, I., (2021). 6G-Enabled Network in Box for Internet of Connected Vehicles, *IEEE Transactions on Intelligent Transportation Systems*, 22-8, 5275-5282.

- [6] Xu, X., Yao, L., Bilal, M., Wan, S., Dai, F. and Choo, K.-K.R., (2022). Service Migration Across Edge Devices in 6G-Enabled Internet of Vehicles Networks, *IEEE Internet of Things Journal*, 9-3, 1930-1937.
- [7] Pan, Q., Wu, J., Nebhen, J., Bashir, A.K., Su, Y. and Li, J., (2022). Artificial Intelligence-Based Energy Efficient Communication System for Intelligent Reflecting Surface-Driven VANETs, *IEEE Transactions on Intelligent Transportation Systems*, 23-10, 19714-19726.
- [8] Tang, F., Kawamoto, Y., Kato, N. and Liu, J., (2020). Future Intelligent and Secure Vehicular Network Toward 6G: Machine-Learning Approaches, *Proceedings of the IEEE*, 108-2, 292-307.
- [9] Noor-A-Rahim, M., Liu, Z., Lee, H., Khyam, M.O., He, J., Pesch, D., Mousser, K. and Poor, H.V., (2022). 6G for Vehicle-to-Everything (V2X) Communications: Enabling Technologies, Challenges, and Opportunities, *Proceedings of the IEEE*, 110-6, 712-734.
- [10] Boulogeorgos, A.-A.A., Sofotasios, P.C., Selim, B., Muhaidat, S., Karagiannidis, G.K. and Valkama, M., (2016). Effects of RF Impairments in Communications Over Cascaded Fading Channels, *IEEE Transactions on Vehicular Technology*, 65-11, 8878-8894.
- [11] Zhang, H., Liao, Z., Shi, Z., Yang, G., Dou, Q. and Ma, S., (2022). Performance Analysis of MIMO-HARQ Assisted V2V Communications with Keyhole Effect, *IEEE Transactions on Communications*, 70-5, 3034-3046.
- [12] Aliev, R., Hehn, T., Kwoczek, A. and Kürner, T., (2018). Predictive Communication and Its Application to Vehicular Environments: Doppler-Shift Compensation, *IEEE Transactions on Vehicular Technology*, 67-8, 7380-7393.
- [13] Karagiannidis, G.K., Sagias, N.C., and Mathiopoulos, P.T., (2007). N\*Nakagami: A novel stochastic model for cascaded fading channels, *IEEE Transactions on Communications*, 55-8, 1453-1458.
- [14] Jaiswal, N. and Purohit, N., (2021). Performance Analysis of NOMA-Enabled Vehicular Communication Systems with Transmit Antenna Selection Over Double Nakagami-m Fading, *IEEE Transactions on Vehicular Technology*, 70-12, 12725-12741.
- [15] Zhang, C., Ge, J., Li, J. and Hu, Y., (2013). Performance analysis for mobile relay-based M2M two-way AF relaying in N\* Nakagami-m fading, *Electronics Letters*, 49-5, 344-346.
- [16] Ata, S.Ö. And Altunbaş, I., (2016). Fixed-gain AF PLNC over cascaded Nakagami-m fading channels for vehicular communications, *AEU-International Journal of Electronics and Communications*, 70-4, 510-516.

- [17] Eshteiwi, K., Sleim, B. and Kaddoum, G., (2020). Full Duplex of V2V Cooperative Relaying over Cascaded Nakagami-m Fading Channels, International Symposium on Networks, Computers, and Communications, Montreal, Canada, 1-5.
- [18] Baek, S., Lee, I. and Song, C., (2019). A New Data Pilot-Aided Channel Estimation Scheme for Fast Time-Varying Channels in IEEE 802.11p Systems, IEEE Transactions on Vehicular Technology, 68-5, 5169-5172.
- [19] Xu, C., An, J., Bai, T., Sugiura, S., Maunder, R.G., Wang, Z., Yang, L.L., Hanzo, L., (2023). Channel Estimation for Reconfigurable Intelligent Surface Assisted High-Mobility Wireless Systems, IEEE Transactions on Vehicular Technology, 72-1, 718-734.
- [20] Liu, T.-H., (2015). Analysis of the Alamouti STBC MIMO System with Spatial Division Multiplexing Over the Rayleigh Fading Channel, IEEE Transactions on Wireless Communications, 14-9, 5156-5170.
- [21] Khattabi, Y.M. and Matalgah, M.M., (2018). Alamouti-OSTBC Wireless Cooperative Networks With Mobile Nodes and Imperfect CSI Estimation, IEEE Transactions on Vehicular Technology, 67-4, 3447-3456.
- [22] Zhu, J., Xiao, L., Xiao, P., Quddus, A., He, C. and Lu, L., (2021). Differential STBC-SM Scheme for Uplink Multi-User Massive MIMO Communications: System Design and Performance Analysis, IEEE Transactions on Vehicular Technology, 70-10, 10236-10251.
- [23] Alamouti, S.M., (1998). Simple Transmit Diversity Technique for Wireless Communications, IEEE Journal on Selected Areas in Communications, 16-8, 1451-1458.
- [24] Gradshteyn, I.S. and Ryzhik, I.M., (2015). Table of Integrals, Series, and Products, 8th ed., Academic Press, New York.
- [25] Prudnikov, A.P., Brychkov, Y.A. and Marichev, O.I., (1986). Integrals and Series - Vol. 3 - More Special Functions. CRC Press.
- [26] Simon, M. K. and Alouini, M.S., (2005). Digital Communication over Fading Channels, 2nd ed., Wiley & Sons.
- [27] Mckay, M.R., Zanella, A., Collings, I.B. and Chiani, M., (2009). Error probability and SINR analysis of optimum combining in rician fading, IEEE Transactions on Communications, 57-3, 676-687.
- [28] Yilmaz, F. and Alouini, M.S., (2012). A Unified MGF-Based Capacity Analysis of Diversity Combiners over Generalized Fading Channels, IEEE Transactions on Communications, 60-3, 862-875.